A Nonlinear Block Structure Identification Procedure Using Frequency Response Function Measurements

Lieve Lauwers, *Member, IEEE*, Johan Schoukens, *Fellow, IEEE*, Rik Pintelon, *Fellow, IEEE*, and Martin Enqvist

Abstract—Based on simple Frequency Response Function (FRF) measurements, we give the user some guidance in the selection of an appropriate nonlinear block structure for the system to be modeled. The method consists in measuring the FRF using a Gaussian-like input signal and varying in a first experiment the root-mean-square (rms) value of this signal while maintaining the coloring of the power spectrum. Next, in a second experiment, the coloring of the power spectrum is varied while keeping the rms value constant. Based on the resulting behavior of the FRF, an appropriate nonlinear block structure can be selected to approximate the real system. The identification of the selected block-oriented model itself is not addressed in this paper. A theoretical analysis and two practical applications of this structure identification method are presented for some nonlinear block structures.

Index Terms—Frequency-domain analysis, frequency response, linear approximation, modeling, nonlinear systems.

I. INTRODUCTION

MODELS built from observed input/output data are widely used to describe, control, and improve systems or processes in different engineering branches, such as chemical, mechanical, civil, and power engineering, signal processing, etc. Since most real-life systems are not linear, their nonlinear behavior needs to be taken into account when performing measurements or designing and calibrating measurement instruments. For this reason, nowadays, nonlinear models have become increasing important for the measurement engineer. Another application of nonlinear modeling is the calibration of nonlinear sensors.

In nonlinear system identification, the selection of an appropriate nonlinear model structure is a first critical step. However, there exists a large variety among nonlinear model structures, e.g., block-oriented models, least squares support vector machines, artificial neural networks, and nonlinear state-space models. We will focus on block-oriented model structures, which have the advantage of giving the user physical insight

into the system under test. A main disadvantage is the difficulty of selecting a suitable model structure that can grasp both the linear dynamic and the nonlinear behavior. For instance, can a simple open loop structure describe the system, or do we need to include a nonlinear feedback? In some cases, the structure of the system under test is known in advance. Then, only the parameters of the block-oriented model structure remain to be estimated. This second step of the identification process is beyond the scope of this paper and will not be addressed here. When no prior knowledge is available, it might be hard for the user to know whether the selected block structure is appropriate for modeling the system. Therefore, a method is required that gives the user some guidance in her/his choice of nonlinear block structures.

Block structure identification methods that detect the structure of a system have already been investigated in the past. Various approaches exist to distinguish between a limited set of structures belonging to a rather small subclass of the block-oriented model class, namely structures consisting of linear dynamic and nonlinear static blocks. One approach is based on the estimated Volterra kernels: Some block structures correspond to a specific (analytical or graphical) interrelationship between the system kernels [1]–[3]. In the frequency method [1], the structure is determined from the pole/zero configuration of the transfer function obtained by applying a harmonic test signal. Another approach uses a correlation analysis: From the linear and nonlinear cross-correlation functions, some block-oriented structures can be distinguished among a predefined set of possibilities [1]. It is important to notice that in each of the aforementioned block structure identification methods, some estimation procedure needs to be performed prior to the model structure selection: a nonlinear model needs to be identified. A last method is based on the results from a two-stage relay feedback experiment: From the duration of the positive and negative errors and the (a)symmetry of the output errors, a distinction can be made between a limited class of model structures containing linear dynamics and memoryless nonlinearities [4].

In this paper, we present a more general approach to discriminate between various subclasses of block-oriented model structures, including different types of nonlinear dynamic blocks and feedback structures. This block structure identification method is based on the behavior of the Frequency Response Function (FRF) of the nonlinear system excited by a Gaussian-like input (i.e., the best linear approximation [5], [6]), as a function of the root-mean-square (rms) value and the coloring of the input signal. Hence, no nonlinear model needs to be identified; only simple linear FRF measurements are needed. All experiments

can thus be performed with the existing dynamic signal analyzers that are commercially available.

This paper is organized as follows: First, the best linear approximation of a nonlinear system is defined for a given class of excitation signals. Next, the nonlinear structure identification procedure is explained in detail. Furthermore, the behavior of the best linear approximation for some nonlinear block structures is described; the theoretical proofs are given in the Appendix. Finally, the method is applied to two different physical systems, and the results are discussed.

II. BEST LINEAR APPROXIMATION

The Best Linear Approximation G_{BLA} of a nonlinear system is optimal in the sense that it minimizes the mean square error between the true output and the modeled output for a particular class of inputs, i.e.,

$$G_{\text{BLA}} = \arg \min_G E\left\{ [y(t) - G(q)u(t)]^2 \right\} \qquad (1)$$

with $u(t)$ and $y(t)$ the measured input and output, respectively, and $G(q)$ the linear transfer function model, where q is the shift operator. Note that this corresponds to the classical FRF measurements based on auto-power and cross-power spectra measurements [7] that are implemented in all commercial dynamic signal analyzers. Thus

$$G_{\text{BLA}}(j\omega) = \frac{S_{yu}(j\omega)}{S_{uu}(j\omega)}. \qquad (2)$$

In (2), $S_{yu}(j\omega)$ is the cross-power spectrum between the output y and the input u, and $S_{uu}(j\omega)$ is the auto-power spectrum of the input [8, Th. 1].

A nonlinear system can always be represented by its best linear approximation G_{BLA} followed by a noise source representing the unmodeled nonlinear contributions of the system [8], [9]. These nonlinear contributions depend on the particular realization of the input signal, and they exhibit a stochastic behavior if the input is a random process. In practice, G_{BLA} can be estimated by averaging the measured FRFs for different input realizations.

The best linear approximation depends on the probability density function (e.g., normal, uniform, or binary distribution) of the excitation signal. We restrict ourselves to the class of Gaussian(-like) excitations. A special member of this class is a random phase multisine, which is defined as

$$u(t) = \sum_{k=1}^{N} U_k \cos\left(2\pi \frac{f}{N} kt + \phi_k\right) \qquad (3)$$

where both the amplitudes U_k and the basis frequency $f_o = f/N$ can be chosen by the user. The phases ϕ_k are independent random variables such that $E\{e^{j\phi_k}\} = 0$. For example, this condition is satisfied when ϕ_k is uniformly distributed over $[0, 2\pi]$. Although, in theory, the number of frequencies N should tend to infinity for a random multisine to become Gaussian, in practice, $N > 20$ already works very

well for smoothly varying amplitude distributions U_k [5], [8]. It should be pointed out that even nonlinearities (e.g., $y = x^2$) do not contribute to G_{BLA}. They only result in a stochastic contribution on both the even and odd frequency lines, which disappears in the averaging process. Hence, the impact on FRF measurements is very similar to disturbing noise. However, by exciting only the odd frequency lines, even nonlinearities will no longer give a contribution on these odd lines where the FRFs are measured [5]. Hence, a lower variance is obtained for G_{BLA} without affecting its value when the excitation signal is an odd multisine (i.e., a random phase multisine with an odd harmonic grid).

III. NONLINEAR STRUCTURE IDENTIFICATION PROCEDURE

The proposed structure identification procedure is based on the fact that G_{BLA} depends on the power spectrum (rms value and coloring) of the input signal [5]. The approach of this method consists in applying a Gaussian-like input signal and varying in a first series of experiments the amplitude or rms value of this signal while maintaining the shape of the power spectrum. Next, in a second series of experiments, the shape of the power spectrum is varied while keeping the rms level constant. The latter is achieved by normalizing the power of the excitation signal before applying it to the system. According to the resulting changes (a vertical shift or a shape change) of the amplitude and phase characteristics of the best linear approximation, an analysis can be made about the appropriateness or ability of some nonlinear block structures to identify the system under test. However, there is no guarantee that there will be a unique solution: In some cases, multiple structures behave similarly. The aim of this method is to give the user some guidance in the choice of nonlinear model structures, not to make a complete and strict classification of nonlinear model structures based on the behavior of their best linear approximation. Furthermore, it should be emphasized that a candidate model structure depends on the rms and color variations applied to the input signal for the structure identification procedure. Consequently, a candidate model structure will only be appropriate to identify the system under test for the range wherein the excitation was modified. Therefore, the user should always apply variations that cover the full amplitude range and frequency band of interest. Within this restricted range, two different model structures may behave similarly, whereas outside this range, their behavior can significantly differ.

IV. SOME NONLINEAR BLOCK STRUCTURES

Block-oriented nonlinear systems are composed of serial and/or parallel connections of linear dynamic blocks and static or dynamic nonlinear blocks. In this section, some block-oriented nonlinear systems that can be distinguished by the proposed method are described. Their best linear approximation, as defined in (2), is studied for the class of Gaussian excitation signals. Here, only the results are presented, whereas the proofs are given in the Appendix.
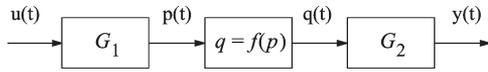
Fig. 1. Wiener–Hammerstein system.

A. Wiener–Hammerstein (WH)

A WH system consists of two linear dynamic systems G_1 and G_2 with a static nonlinearity (SNL) $f(p)$ in between (see Fig. 1). The signals $u(t)$ and $y(t)$ are the system input and output, respectively; $p(t)$ and $q(t)$ are internal signals that are not measurable.

For WH systems, different excitation levels of the input signal $u(t)$ give a vertical shift in the amplitude of the best linear approximation G_{BLA}, without a change in its phase. Special cases of the WH system are a Wiener (W) and a Hammerstein (H) system in which, respectively, the last filter G_2 and the first filter G_1 is set to 1. The best linear approximation of a Wiener system behaves exactly like the one of a WH system. The G_{BLA} of a Hammerstein system shows the same behavior when varying the rms value of the input signal. However, when the bandwidth is modified, its characteristics do not change, whereas this is the case for a Wiener and a WH system. The proofs of these results can be found in Appendix B.

B. Wiener–Hammerstein-NFIR (WH-NFIR)

A WH system where the SNL is replaced by a dynamic nonlinearity with a finite memory is called a WH-Nonlinear Finite-Impulse-Response (WH-NFIR) system. Now, the output $q(t)$ of the nonlinear element depends not only on the present input but also on a finite number of past inputs. Hence, such a system can be written as

$$q(t) = f\left(p(t), p(t-1), \ldots, p(t-M)\right) \qquad (4)$$

where f is a nonlinear function. For this system, two types of nonlinearities can be distinguished: a polyNFIR and an NFIRsum.

In a WH-polyNFIR system, the dynamic nonlinearity consists of a monomial, i.e., one term of a polynomial

$$q(t) = c \cdot \prod_{i=0}^{M} p^{\beta_i}(t-i) \qquad (5)$$

where c is a constant, and $\beta_i \in \mathbb{R}^+$. Varying the rms value of the input signal gives rise to a shift in the amplitude of G_{BLA} of WH-polyNFIR systems, whereas the phase remains unchanged. Varying the shape of the power spectrum results in shape changes of both the amplitude and phase characteristics of G_{BLA}. These results are proven in Appendices A2a and C1.

In a WH-NFIRsum system, the dynamic nonlinearity can be written as

$$q(t) = \sum_{i=0}^{M} g_i\left(p(t-i)\right) \qquad (6)$$

i.e., a sum of nonlinear functions g_i with only one argument. For these systems, the best linear approximation changes
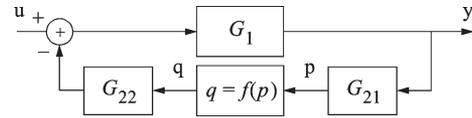

Fig. 2. Nonlinear Feedback system.

TABLE I
GENERAL BEHAVIOR OF THE BEST LINEAR APPROXIMATION OF SOME NONLINEAR SYSTEMS. ↗ STANDS FOR A VERTICAL SHIFT, = MEANS THAT NOTHING CHANGES, AND Δ DENOTES A FREQUENCY-DEPENDENT CHANGE

	Gaussian excitation signals			
	changing rms value		changing colouring	
	$\lvert G_{BLA}\rvert$	$\angle G_{BLA}$	$\lvert G_{BLA}\rvert$	$\angle G_{BLA}$
WH, W	↗	=	↗	=
H	↗	=	=	=
WH-polyNFIR	↗	=	Δ	Δ
H-NFIRsum	Δ	Δ	=	=
W(H)-NFIRsum	Δ	Δ	Δ	Δ
NLFB	Δ	Δ	Δ	Δ

in shape when the rms value or the coloring of the power spectrum of the input signal is varied. In the special case of an H-NFIRsum system, the best linear approximation stays invariant when modifying the bandwidth. These results are proven in Appendices A2b and C2.

C. Nonlinear Feedback (NLFB)

In NLFB systems with a WH structure (containing an SNL) in the feedback loop (see Fig. 2), it can be shown that variations of the input signal (rms and coloring) lead to shape changes of both the amplitude and phase of the best linear approximation [11]. This corresponds to a pole displacement, which is consistent with the system and control theory.

D. Summary

The aforementioned results are summarized in Table I.

According to the behavior of their best linear approximation, model structures can be divided into different classes, in which the structures show the same behavior. If the measured behavior of the system under test corresponds to one of the classes, all the structures in that class are good candidates to approximate the true system. Structures outside that class show a different behavior and, thus, are less appropriate to model the system. From Table I, we can distinguish five classes of nonlinear model structures with a different behavior for the best linear approximation: 1) W(H) systems; 2) H systems; 3) WH-polyNFIR systems; 4) H-NFIRsum systems; and 5) the general class including W(H)-NFIRsum systems and NLFB systems. Since WH-NFIRsum structures and NLFB structures belong to the same class, they cannot be distinguished from each other based on the characteristics of their best linear approximation. As a result, a WH-NFIRsum structure might be used as an approximate model structure to identify an NLFB system,
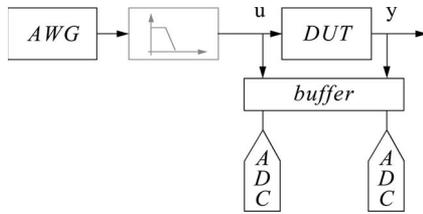
Fig. 3. Experimental setup for the Silverbox and the crystal detector (black). A low-pass filter (gray) is added in the Silverbox case study.

although it does not correspond to the true structure of the system.

V. EXPERIMENTS AND RESULTS

To illustrate its user friendliness, ease, and wide scope, the structure identification method described in Section III is applied to two physical systems in various domains. The first system is an electrical circuit simulating the behavior of a nonlinear mass–spring–damper system, which is also known as the "Silverbox" [12]. The second system is an Agilent-HP420C crystal detector, which is a device used for microwave power measurements.

The measurement setup for both case studies is shown in Fig. 3 and consists of an Arbitrary Waveform Generator (AWG; HP E1445A, 13-bit resolution, memory length of 256 000 samples), the Device Under Test (DUT), a buffer, and two Analog-to-Digital Converters (ADCs; HP E1430A). The AWG and ADCs are part of an Agilent VXI high-power mainframe (E1401B). The input signal is generated by the AWG, which is connected to a computer via an IEEE-1394 link. For the Silverbox measurements, a low-pass reconstruction filter (Difa PDF 3700 with a cutoff frequency of 300 Hz) is set after the AWG. Due to the zero-order-hold reconstruction of the AWG, unwanted spectral repetitions of the input spectrum appear at higher frequencies around multiples of the sampling frequency. Due to the mixing behavior of the nonlinear device, these repetitions can interfere with the frequency band of interest and, hence, need to be removed using an analog reconstruction filter. For the crystal detector, the sampling frequency is set to its maximum value (10 MHz). Then, no reconstruction filter is needed because of the limited intrinsic bandwidth of the AWG. Finally, the input and output of the DUT are measured using two ADCs, which are placed after a buffer with a high input impedance.

A. Silverbox

The Silverbox was excited with a random odd multisine, i.e., an odd multisine where, in every set of three consecutive odd frequency lines, one line is randomly set to zero. In a first experiment, this input signal was applied to the system at different rms levels (21.8, 43.6, 87.3, and 348.6 mV). The input and output were measured with a sample frequency of 1220.7 Hz. For each rms level, 128 phase realizations, composed of two periods of 2048 data points each, were applied to the Silverbox. The measured input and output signals were averaged over the two periods, and next, the best linear approximation was
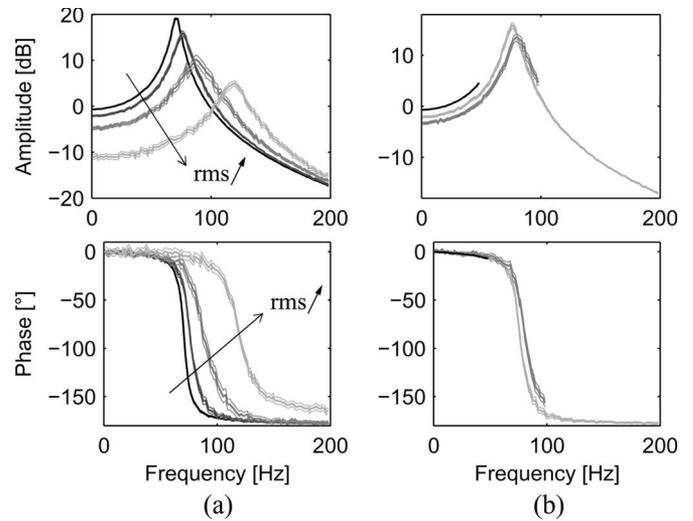

Fig. 4. Behavior of G_{BLA} (bold lines) and its 95% uncertainty bounds (thin lines) for (a) different rms values and (b) different bandwidths. Top figures: Amplitude FRF. Bottom figures: Phase FRF.

nonparametrically estimated by averaging the measured FRFs over the 128 different phase realizations. Furthermore, the total standard deviation (including the disturbing noise and the stochastic nonlinear distortions [13]) on the best linear approximation G_{BLA} was calculated. The amplitude and phase of G_{BLA} are plotted in Fig. 4(a) for the different rms levels (bold lines), together with the 95% uncertainty bounds (thin lines). From these plots, we see that both the amplitude and phase of the best linear approximation change: they shift to the right for larger rms values. These shape changes are statistically significant within the 95% confidence bounds since these bounds do not coincide for the different rms values. Note that for growing amplitudes of the input signal, G_{BLA} becomes less smooth. This is due to the fact that the nonlinearities in the system are more excited and become dominant. Hence, more averages are needed to obtain a smoother FRF measurement.

In a second experiment, the coloring of the power spectrum of the input signal was varied while keeping the rms value constant. In Fig. 4(b), the behavior of G_{BLA} (bold lines) is shown for different bandwidths (50, 100, and 200 Hz), together with the 95% confidence bounds (thin lines). In the full band (up to 200 Hz), we observe a statistically significant shape change of both the amplitude and phase of G_{BLA} when varying the bandwidth of the excitation signal.

By combining the results from both experiments, we conclude from Table I that there are two candidate model structures for the Silverbox: a W(H)-NFIRsum structure and an NLFB structure. So far, the first model structure is not tried out to model this system. In [14], an NLFB framework was successfully utilized. This confirms the ability of the proposed feedback structure to identify the Silverbox. Note that if the user is only interested in identifying this system in a frequency band up to 50 Hz, a W(H) structure is a good candidate model structure since the amplitude of G_{BLA} shifts vertically, whereas the phase does not significantly change when varying the power spectrum in this frequency band.
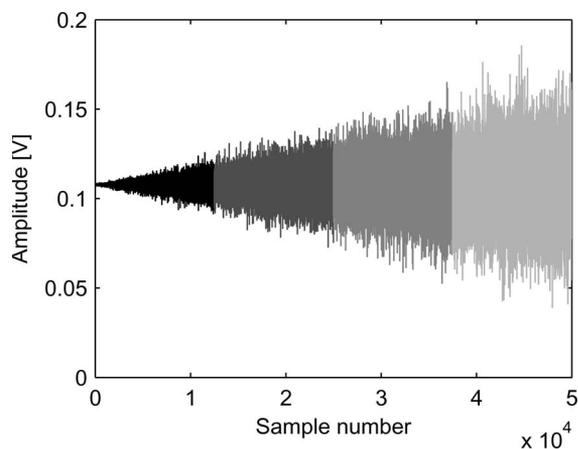
Fig. 5.   Arrowlike signal segmented into four blocks.

Fig. 6.   Behavior of G_{BLA} (bold lines) and its 95% uncertainty bounds (thin lines) for (a) different rms values and (b) different bandwidths. Top figures: Amplitude FRF. Bottom figures: Phase FRF.

B. Crystal Detector

In the second case study, a crystal detector was excited with a nonstationary Gaussian signal with a slowly growing amplitude (see Fig. 5). This noise sequence consisted of 50 000 data points and was repeated five times. The input and output were measured with a sampling frequency of 10 MHz.

In a first experiment, the amplitude and phase characteristics of G_{BLA} are investigated for different rms levels. For this, the excitation signal was averaged over the five periods and then divided into four blocks of 12 500 points, so that each block corresponds to a different rms value. Next, for every segment of the arrowlike signal (see Fig. 5), the best linear approximation was estimated by dividing each segment into 100 equal blocks. Due to the nonstationary behavior of the Gaussian excitation, the total standard deviation on G_{BLA} could not precisely be calculated. In order to have an idea of the 95% uncertainty bounds, an overestimate of the standard deviation was determined. Therefore, the standard deviation was calculated on G_{BLA} estimated from the last 1250 data points of a segment, which were split into ten equal blocks. The resulting standard deviation was then scaled up to the whole segment according to the $\sqrt{N}$ law. In order not to overload the plots, we only show in Fig. 6(a) the best linear approximation of the first and last segments (bold lines), which correspond to the lowest and largest rms values, respectively. The overestimated 95% uncertainty bounds are also plotted (thin lines), but they can hardly be seen. From these 95% confidence bounds, we observe a statistically significant variation of both the amplitude and phase of G_{BLA} when the rms level of the input signal is altered.

In a second experiment, the behavior of G_{BLA} is examined when changing the shape of the power spectrum of the input signal. For this, the Gaussian noise sequence was first pre-filtered by a second-order Butterworth filter, then normalized to keep the rms level unchanged, and, finally, applied five times to the DUT. The Butterworth filter was designed at two different cutoff frequencies: 400 and 800 kHz. For each cutoff frequency, the arrowlike signal (averaged over the five periods) is again split into several segments. Next, the best linear approximations of segments with the same rms value but
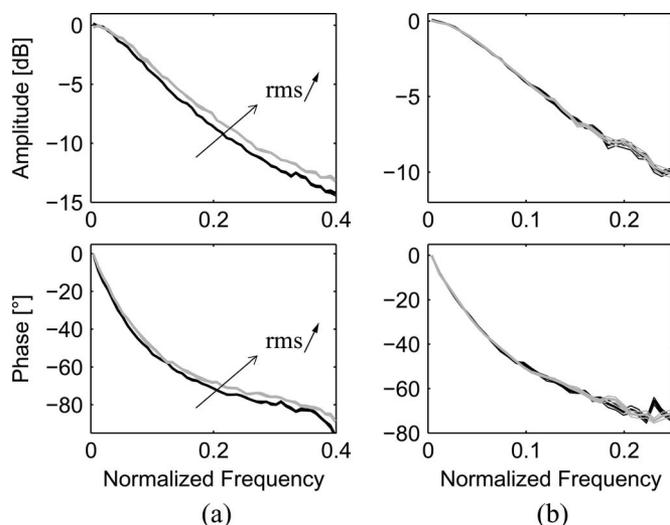
originating from differently colored input signals are compared. The resulting amplitude and phase characteristics of G_{BLA} for the first segments are shown in Fig. 6(b) (bold lines), together with the (overestimated) 95% uncertainty bounds (thin lines). From these plots, we observe no significant variation in G_{BLA}, neither in its amplitude nor in its phase.

By comparing the experimental results in Fig. 6 with Table I, we can conclude that an H-NFIRsum structure is a possible candidate to model the DUT. This structure corresponds to a shape change of both the amplitude and phase when the rms level of the input is varied, whereas the characteristics of G_{BLA} do not change when the coloring of the input is modified. Note that if we would further vary the shape of the power spectrum, we might see a significant shape change in the characteristics of G_{BLA}. If so, an NLFB structure and a WH-NFIRsum system are good candidates.

VI. CONCLUSION

A structure identification method based on the best linear approximation for the distinction between various subclasses of block-oriented model structures was presented, theoretically analyzed, and illustrated by two practical examples. For each case study, specific block structures were pointed out as being appropriate to identify the system under test in the frequency band and amplitude range wherein the input signal was varied. We showed that this method is applicable in various fields and easy to implement since the user only needs to carry out FRF measurements, together with a variance analysis. Using this two-stage nonparametric approach, the user immediately obtains insight in the ability of some nonlinear block structures to model the system under test, without any parameter estimation. Hence, this method provides a valuable tool for the measurement and test engineer to obtain a better insight in the structure of her/his problem at hand, using well-known classical measurement methods.

Appendix

In this section, the resulting behavior of the best linear approximation for several block-oriented systems when changing the power spectrum of the input signal is theoretically proven. In Appendix A, the system consists only of a static or a dynamic nonlinearity. This corresponds to a WH structure, where $G_1 = G_2 = 1$, so that $p = u$ and $q = y$. In Appendix B and C, this nonlinearity is inserted into a WH structure.

A. Different Types of Nonlinearities

1) SNL: The best linear approximation of an SNL is a scale factor that depends on the rms level of the input of the nonlinear block for Gaussian excitation signals [5], [6]. As a result, different amplitude levels of the input signal induce a vertical shift in the amplitude of G_{BLA}, without a change in its phase. Different bandwidths of the excitation do not at all influence the characteristics of G_{BLA}.

2) NFIR System: The following generalization of Bussgang's theorem for NFIR systems with Gaussian input signals will be used.

Theorem: Let $y(t) = f(u(t), u(t-1), \ldots, u(t-M))$ be an NFIR system with a stationary Gaussian $u(t)$ process as input. Assume that the expectations $E\{u(t)\} = E\{y(t)\} = 0$. Then, it follows that

$$R_{yu}(\tau) = \sum_{k=0}^{M} b(k) R_{uu}(\tau - k) \qquad \forall \tau \in \mathbb{Z} \qquad (7)$$

where

$$b(k) = E\left\{ \frac{\partial f}{\partial u_k} \right\} \qquad (8)$$

with $u_k = u(t-k)$, $R_{yu}(\tau) = E\{y(t)u(t-\tau)\}$ the cross-covariance function between the output and the input, and $R_{uu}(\tau) = E\{u(t)u(t-\tau)\}$ the auto-covariance function of the input.

Proof: See [6].

Using the Z-transform, (7) can be written as $S_{yu}(z) = B(z)S_{uu}(z)$, where $B_z = \sum_{k=0}^{M} b(k)z^{-k}$. From this equation, it follows that the best linear approximation, in mean square sense, of an NFIR system with a Gaussian input is the linear Finite-Impulse Response (FIR) model, i.e.,

$$G_{\mathrm{BLA}}(z) = \frac{S_{yu}(z)}{S_{uu}(z)} = \sum_{k=0}^{M} b(k)z^{-k}. \qquad (9)$$

This relation will be used to characterize the G_{BLA} of an NFIR system with a Gaussian input when the power spectrum of the input is shifted or shaped. We distinguish two types of NFIR systems: polyNFIR and NFIRsum.

a) PolyNFIR: $y(u(t)) = c \cdot \prod_{i=0}^{M} u^{\beta_i}(t-i)$

- Changing rms: When the amplitude or rms level of the input signal $u(t)$ is multiplied by γ, the general formula (5) of a polyNFIR system can be rewritten as

$$y(\gamma u(t)) = \gamma^{\sum_i \beta_i} y(u(t)) \qquad (10)$$

where γ is the rms value.

Using (8) and (10), the $b_\gamma(k)$ coefficients before $(\gamma = 1)$ and after $(\gamma \neq 1)$ changing the rms value can be calculated. It follows immediately that

$$b_\gamma(k) = \alpha(\gamma)b_1(k), \qquad \forall k$$

$$\text{where } \alpha(\gamma) = \gamma^{\sum_i \beta_i - 1} \qquad (11)$$

and thus, $B_\gamma(z) = \alpha(\gamma)B_1(z)$. As a result, the amplitude of G_{BLA} will vertically shift by a scale factor $\alpha(\gamma)$, whereas the phase remains unchanged when the rms value of the Gaussian input is altered.

- Changing coloring: When colored Gaussian noise is used to excite the system, the input signal $u(t)$ can be written as filtered white zero-mean Gaussian noise $e(t)$ with variance σ^2, i.e.,

$$u(t) = \sum_{s=0}^{\infty} h(s)e(t-s) \qquad (12)$$

with $h(t)$ the impulse response of the coloring filter. Consider a polyNFIR system $y(t) = u(t)u^2(t-1)$. The best linear approximation of this system will be according to (9):

$$G_{\mathrm{BLA}}(z) = b(0) + b(1)z^{-1} \qquad (13)$$

where $b(0) = \sigma^2 R_{hh}(0)$ and $b(1) = 2\sigma^2 R_{hh}(1)$. Here, R_{hh} denotes $R_{hh}(\tau) = \sum_{s=0}^{\infty} h(s)h(\tau - s)$. If the input is white noise, these expressions reduce to $b(0) = \sigma^2$ and $b(1) = 0$. This example shows that the $b(k)$ coefficients are, in general, not equal for white and colored noise, since $b(k)$ depends on the bandwidth of the input signal. Consequently, both the amplitude and phase of G_{BLA} change when the power spectrum of the excitation signal is shaped.

- Generalization: It can be proven that the same properties for the best linear approximation hold for homogeneous polynomials (i.e., polynomials where the degrees of all terms are equal). Varying the rms level of the input results in a vertical shift of the amplitude, without a change of the phase, whereas modifying the bandwidth of the input signal leads to shape changes of both the amplitude and phase.

b) NFIRsum: $y(t) = \sum_{i=0}^{M} g_i(u(t-i))$

- Changing rms: For an NFIRsum system, every $b(k)$ coefficient depends on the partial derivative of a different function g_k with respect to u_k, i.e.,

$$b(k) = E\{g'_k(u_k)\} \qquad (14)$$

with $g'_k(u_k) = (d/du_k)g_k(u_k)$. In general, the arbitrary functions g_i are nonlinear, which implies that $g_i(\gamma u_i) \neq \gamma g_i(u_i)$. Thus, every $b_\gamma(k)$ coefficient generally changes in a different way with respect to $b_1(k)$ when the rms value γ is varied. This property can be illustrated with an example. Consider the NFIRsum system $y(t) = u(t) + u^3(t-1)$ and a zero-mean Gaussian input $u(t)$. For this system, the $b_\gamma(k)$ coefficients are (using the chain rule)

TABLE II
GENERAL BEHAVIOR OF THE BEST LINEAR APPROXIMATION OF
SOME NONLINEARITIES. ↗ STANDS FOR A VERTICAL
SHIFT; = MEANS THAT NOTHING CHANGES; AND Δ
DENOTES A FREQUENCY-DEPENDENT CHANGE

	Gaussian excitation signals			
	changing rms value		changing colouring	
	$\lvert G_{BLA} \rvert$	$\angle G_{BLA}$	$\lvert G_{BLA} \rvert$	$\angle G_{BLA}$
SNL	↗	=	=	=
polyNFIR	↗	=	Δ	Δ
NFIRsum	Δ	Δ	=	=

$b\gamma(0) = 1$ and $b\gamma(1) = 3\gamma^2$. These b_γ coefficients differently change as a function of γ. This can be expressed, in general, as $b\gamma(k) = \alpha_k(\gamma)b_1(k)$, where $\alpha_k(\gamma)$ depends on γ and differs for every k. Consequently

$$B\gamma(z) = \sum_{k=0}^{M} \alpha_k(\gamma)b_1(k)z^{-k}. \qquad (15)$$

In conclusion, varying the rms value of the input signal results in a shape change of both the amplitude and phase of B_γ and, thus, G_{BLA}.

- Changing coloring: By definition, $E\{g'_k(u_k)\} = \int g'_k(u_k)p(u_k)du_k$, where $p(u)$ is the probability density function of one component in the zero-mean Gaussian input signal u. Because linear filtered zero-mean Gaussian noise is still zero-mean Gaussian, and because the variance is preserved due to normalization, we have that the expected value does not change. Every $b(k)$ is thus independent of the coloring of the input signal. In other words, neither the amplitude of G_{BLA} nor its phase will vary when the shape of the power spectrum is modified.
- Summary: The theoretical results for the different types of nonlinearities are summarized in Table II.

B. WH System

The best linear approximation G_{BLA} of a WH system (Fig. 1) has already been studied [5]–[10] and can be written as

$$G_{\text{BLA}}(j\omega) = kG_1(j\omega)G_2(j\omega) \qquad (16)$$

where k is the best linear approximation of the SNL depending on the rms value of $p(t)$. When the power spectrum of the input $u(t)$ is varied, a signal $p(t)$ with a different rms value and coloring generally appears at the input of the SNL. This is due to the presence of the first filter G_1. As a result, the amplitude of G_{BLA} for WH systems vertically shifts, whereas its phase stays invariant.

Since the presence of the last filter G_2 does not influence the behavior of G_{BLA}, a Wiener system (for which $G_2 = 1$ holds) exactly behaves like a WH system. On the other hand, the characteristics of G_{BLA} for a Hammerstein system (where $G_1 = 1$) match those of the SNL.

C. WH-NFIR System

A WH-NFIR system is a WH system where the SNL is replaced by an NFIR subsystem. The best linear approximation of such a system for a Gaussian input is given by

$$G_{\text{BLA}}(z) = G_2(z)B(z)G_1(z) \qquad (17)$$

where $B(z) = \sum_{k=0}^{M} b(k)z^{-k}$ is the approximating FIR model of the NFIR system from $p(t)$ to $q(t)$ [6], [9]. Relation (17) will be used to prove the resulting changes of G_{BLA} when the power spectrum of the Gaussian input is varied.

1) WH-polyNFIR:

- Changing rms: When the rms level γ of the input signal $u(t)$ is modified, G_{BLA} in (17) will change according to the best linear approximation $B(z)$ of the polyNFIR system. Since the equality $B\gamma(z) = \alpha(\gamma)B_1(z)$ holds in this case, WH-polyNFIR systems have the property that different rms values γ give a vertical shift in the amplitude of G_{BLA}, without a change in its phase.
- Changing coloring: When the bandwidth of the excitation signal $u(t)$ is modified while keeping its rms value constant, a signal $p(t)$ with a different power spectrum appears at the input of the polyNFIR system. This is due to the filtering effect of the linear dynamic block G_1. Since the best linear approximation $B(z)$ of a polyNFIR system depends on the power spectrum of $p(t)$, it follows that the G_{BLA} of a WH-polyNFIR system changes in amplitude and phase when the coloring of the input signal $u(t)$ is varied.

2) WH-NFIRsum:

- Changing rms: In Appendix A2b, we proved that the best linear approximation $B(z)$ of an NFIRsum system shows shape changes of both the amplitude and phase when varying the rms value of the input signal. As a result, G_{BLA} in (17) will accordingly change so that the same property holds for WH-NFIRsum systems.
- Changing coloring: When the coloring of the input signal $u(t)$ is varied while maintaining its rms value, a signal $p(t)$ with a different rms value and coloring will generally appear at the input of the NFIRsum system. This is due to the presence of the first filter G_1. Since the best linear approximation $B(z)$ of an NFIRsum system depends on the rms level of $p(t)$, the G_{BLA} of a WH-NFIRsum system changes in shape when the power spectrum of the input signal $u(t)$ is modified.

REFERENCES

[1] R. Haber and H. Unbehauen, "Structure identification of nonlinear dynamic systems—A survey on input/output approaches," *Automatica*, vol. 26, no. 4, pp. 651–677, Jul. 1990.
[2] H.-W. Chen, "Modeling and identification of parallel nonlinear systems: Structural classification and parameter estimation methods," *Proc. IEEE*, vol. 83, no. 1, pp. 39–66, Jan. 1995.
[3] M. Weiss, C. Evans, D. Rees, and L. Jones, "Structure identification of block-oriented nonlinear systems using periodic test signals," in *Proc. IEEE Instrum. Meas. Technol. Conf.*, 1996, vol. 1, pp. 8–13.
[4] H.-P. Huang, M.-W. Lee, and C.-Y. Tsai, "Structure identification for block-oriented nonlinear models using relay feedback tests," *J. Chem. Eng. Jpn.*, vol. 34, no. 6, pp. 748–756, 2001.

[5] R. Pintelon and J. Schoukens, *System Identification: A Frequency Domain Approach*. Piscataway, NJ: IEEE Press, 2001.

[6] M. Enqvist, "Linear models of nonlinear systems," Ph.D. dissertation, Linköping Univ., Linköping, Sweden, 2005.

[7] J. S. Bendat and A. G. Piersol, *Engineering Applications of Correlations and Spectral Analysis*. New York: Wiley, 1980.

[8] J. Schoukens, R. Pintelon, T. Dobrowiecki, and Y. Rolain, "Identification of linear systems with nonlinear distortions," *Automatica*, vol. 41, no. 3, pp. 491–504, Mar. 2005.

[9] M. Enqvist and L. Ljung, "Linear approximations of nonlinear FIR systems for separable input processes," *Automatica*, vol. 41, no. 3, pp. 459–473, Mar. 2005.

[10] C. Evans and D. Rees, "Nonlinear distortions and multisine signals—Part I: Measuring the best linear approximation," *IEEE Trans. Instrum. Meas.*, vol. 49, no. 3, pp. 602–609, Jun. 2000.

[11] J. Schoukens, J. Swevers, J. Paduart, D. Vaes, K. Smolders, and R. Pintelon, "Initial estimates for block structured nonlinear systems with feedback," in *Proc. Int. Symp. Nonlinear Theory Appl.*, 2005, pp. 622–625.

[12] J. Schoukens, J. G. Nemeth, P. Crama, Y. Rolain, and R. Pintelon, "Fast approximate identification of nonlinear systems," *Automatica*, vol. 39, no. 7, pp. 1267–1274, Jul. 2003.

[13] T. D'haene, R. Pintelon, J. Schoukens, and E. Van Gheem, "Variance analysis of frequency response function measurements using periodic excitations," *IEEE Trans. Instrum. Meas.*, vol. 54, no. 4, pp. 1452–1456, Aug. 2005.

[14] J. Paduart and J. Schoukens, "Fast identification of systems with nonlinear feedback," in *Proc. 6th IFAC Symp. NOLCOS*, Stuttgart, Germany, 2004, pp. 525–529.

Johan Schoukens (M'90–SM'92–F'97) was born in Belgium in 1957. He received the Engineer degree and the Ph.D. degree in applied sciences from the Vrije Universiteit Brussel (VUB), Brussels, Belgium, in 1980 and 1985, respectively.

He is currently a Professor with the VUB. His main research interest is in the field of system identification for linear and nonlinear systems.

Rik Pintelon (M'90–SM'96–F'98) was born in Gent, Belgium, on December 4, 1959. He received the Burgerlijk Ingenieur degree in electrical engineering, the Ph.D. degree in applied sciences, and the qualification to teach at university level (Geaggregeerde voor het Hoger Onderwijs) from the Vrije Universiteit Brussel (VUB), Brussels, Belgium, in 1982, 1988, and 1994, respectively.

From October 1982 to September 2000, he was a Researcher with the Fund for Scientific Research-Flanders (FWO-Vlaanderen), VUB. Since October 2000, he has been a Professor with the Department of Fundamental Electricity and Instrumentation (ELEC), VUB. His main research interests are in the field of parameter estimation, system identification, and signal processing.

Lieve Lauwers (M'08) was born in Belgium on March 15, 1982. She received the Burgerlijk Ingenieur degree in electrical engineering in 2005 from the Vrije Universiteit Brussel (VUB), Brussels, Belgium, where she is currently working toward the Ph.D. degree.

In August 2005, she joined the Department of Fundamental Electricity and Instrumentation (ELEC), VUB. Her research interests are in the field of nonlinear system identification.

Martin Enqvist was born in Lund, Sweden, in 1976. He received the M.Sc. degree in applied physics and electrical engineering and the Ph.D. degree in automatic control from Linköping University, Linköping, Sweden, in 2000 and 2005, respectively.

In 2006, he was a Postdoctoral Researcher with the Vrije Universiteit Brussel, Brussels, Belgium. He is currently a Research Associate with the Department of Electrical Engineering, Linköping University. His main research interest is in the field of nonlinear system identification.